OPTIMAL MANAGEMENT OF FLEXIBILITY SERVICES IN LV DISTRIBUTION GRIDS

Riccardo NEBULONI, Valentin ILEA, Alberto BERIZZI
Politecnico di Milano – Italy
riccardo.nebuloni@polimi.it

Cristian BOVO
Università degli Studi di Pavia - Italy
cristian.bovo@unipv.it

Carlo ARRIGONI, Franco CORTI, Brunella CONTE
Siemens SpA - Italy
carlo.arrigoni@siemens.com

Roberto BONERA
Freelancer - Italy
roberto.bonera@gmail.com

ABSTRACT

With the increase of intermittent and not programmable generation from clean resources and of new demand technologies characterized by high coincident peaks (like heat pumps, induction cookers, etc.) the management of available flexibility in distribution grids to provide network services has become very important. The paper proposes an optimization model to manage the flexibility in the LV network to both solve local network problems and aggregate the available flexibility for use at higher levels while satisfying LV network constraints. The model is a tool for the LV DSOs to optimally manage the flexibilities and its features are illustrated on the IEEE 123 test feeder.

INTRODUCTION

Currently the European Union (EU) is pushing for de-carbonization (Directive EU 2019/1161): the Renewable Energy Sources (RES) must cover at least 32% of total demand by 2030 while the share of clean vehicles in the total procured must be at least 35% by 2025. A high amount of RES - intrinsically intermittent and not programmable – will be present while a high amount of electric vehicles, together with other types of new electric loads (e.g. heat pumps, induction cookers), will lead to a large part of demands with high coincident peaks. This will make the balancing of generation and demand very challenging, rendering the Ancillary Services Markets (ASM) crucial.

Historically the ASM activates the flexibility of the large, conventional generation connected to HV grid to solve imbalances and HV network security issues. The generators offer their flexibility to alter the production, while the Transmission System Operator (TSO) purchases the needed resources. The accepted bids are valued at the offered price (pay-as-bid). However, the large amount of flexibility from RES and Demand-Side Response (DSR) cannot be ignored anymore by the ASM. The majority is spread in the nodes of the MV and LV distribution networks (DNs) hence it is not feasible to manage them in a centralized, national level, ASM. Also, the security of DNs need to be satisfied when dispatching the flexibility.

In recent years, the focus has been on the MV flexibilities and many approaches were studied from a regulatory, e.g. [1][2] in Italy, or scientific, e.g. [3][4][5], perspective, and by many European projects, e.g. [5][6][7]. A common framework is identified where either (**O1**) the Distribution System Operator (DSO) assures the security of the DN through a local ASM while not unbalancing the HV grid, or (**O2**) **O1** and the DSO also aggregates the technically feasible flexibility to offer it in the centralized ASM. These logics require the flexibility to be aggregated at nodal level which is a complex task given the variety of technologies involved; however, this has been extensively researched in literature, e.g. [8][9][10]. Moreover, these logics involve a separated but coordinated management of flexibility and grids by the TSO and MV DSOs and are practically achievable: while the TSO infrastructure is historically well developed, in recent years there is a strong push to develop the DN infrastructure from calculating its real time state of operation [11][12] to optimally control the flexibility resources to assure MV DN security in terms of voltage and congestions mitigation [13]. These solutions were integrated in Distribution Management Systems (DMS) for MV DSOs, e.g. [14][15]. On top, at regulatory level, efforts are made to progressively integrate the MV flexibility in the ASM market in **O1** or **O2** logic [2].

Plenty of unlocked flexibility is also present at LV level [16], but it has not been sufficiently studied. Clearly, the same management logics as with the MV DNs will work best given the similar characteristics, with the difference that now the interaction is between the MV and LV DSOs instead of between TSO and MV DSO. However, the LV DN is not balanced and symmetrical, so the flexibility managed is more complex. Thus, an innovative methodology to optimally manage the flexibility resources is here proposed for LV networks: a MILP that models the LV DN in details, including a full polyphase representation with mutual coupling and the management of the neutral conductor. The algorithm is a tool for the DSO to correctly assess the impact of flexibility on the electric grid while maximizing its availability to the MV level.

CALCULATION MODEL

Flexibility model

The ownership of the distribution company ends at the Point of Delivery (POD) of energy to the customer where monitoring is also present. Hence, the flexibility available is considered, individually, for each POD. In LV DNs the PODs are mostly single-phase and sometimes three-phase

(Fig 1), so the real and reactive powers initially injected by generic POD, i_{POD}, are $P^0_{ph,i_{POD}}$ and $Q^0_{ph,i_{POD}}$, with $ph = \{a, b, c\}$; injections given by the difference between total generation and demand under the POD. Moreover, since the customers under a POD are linked to the neutral conductor, the sum of the POD injected currents is injected into the neutral conductor (Fig 1).

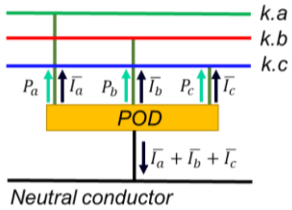

Fig 1: LV POD flexibility representation.

The real power flexibility of each POD is defined using generation convention in the form of a multi-step bid with respect to the total real power injected, $P^0_{i_{POD}} = \sum P^0_{ph,i_{POD}}$, as shown in Fig 2. Each step is characterized by a price and a quantity. Here, also the ON/OFF costs are considered thus both continuous and discrete bids can be modelled. This bid structure corresponds to the actual Italian ASM one.

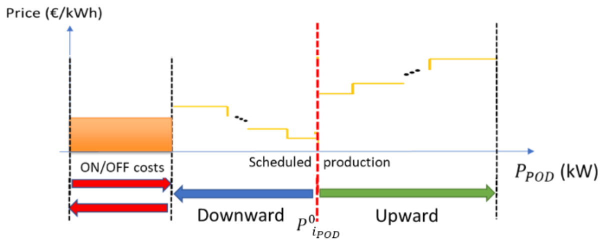

Fig 2: Generic structure of POD flexibility bid.

Thus, the power injected by each POD can be varied as:

$$P_{i_{POD}} = P^0_{i_{POD}} + Y^{UP}_{i_{POD}} \cdot \Delta^{UP}_{0,i_{POD}} - Y^{DW}_{i_{POD}} \cdot \Delta^{DW}_{0,i_{POD}} + \sum_{\forall\, i_{FX} \in\, i_{POD}} P^{UP}_{i_{FX}} - \sum_{\forall i_{FX} \in i_{POD}} P^{DW}_{i_{FX}} \quad (1)$$

where superscripts "UP"/"DW" stand for upward and downward flexibility bids; $Y^{UP\ or\ DW}_{i_{POD}}$ is a binary variable quantifying if the upward or downward bid, respectively, was accepted. The two are complementary, therefore the acceptance of one implies the refusal of the other. Lastly, $P^{UP\ or\ DW}_{i_{FX}}$ is the quantity accepted for each step i_{FX} of the bid, while $P_{i_{POD}}$ is the real power generated by POD i_{POD} following the activation of flexibility. Then, the accepted quantity is assigned to each phase of the POD by:

$$P_{ph,i_{POD}} = P^0_{ph,i_{POD}} + \frac{P_{i_{POD}}}{N} \quad (2)$$

where N is the number of POD's phases. In (2), the bid steps are accepted sequentially, in economic merit order.
Considering the POD operated at constant power factor ($\tan \varphi^0_{i_{POD}}$ = ct.) the reactive power injected by the POD is:

$$Q_{ph,i_{POD}} = \pm P_{ph,i_{POD}} \cdot \tan \varphi^0_{i_{POD}} \quad (3)$$

LV network model

To verify the feasibility of flexibility activation the network's operating constraints need to be checked. The non-linear AC Power Flow (PF) model cannot be used for this inside an optimization problem because it is strongly non-linear while flexibility bids can also be discrete: the resulting optimization problem would be a large mixed integer non-linear program which, by its nature, cannot be solved in reasonable computation time. The very efficient linearized model proposed in [17] has thus been implemented; the main equations are resumed in complex form:

$$\sum_{i_x \in \Omega_x} \boldsymbol{I}^x_{i_x} = \sum_{j \in \Omega_B} \boldsymbol{Y}_{k,j} \cdot \boldsymbol{V}_j,\ x = \{POD, DG, D\} \quad (4)$$

$$\boldsymbol{S}^x_k = \boldsymbol{V}^{0\,\boldsymbol{T}}_k \cdot \boldsymbol{I}^{x*}_k,\ x = \{POD, DG, D\} \quad (5)$$

$$\boldsymbol{I}_{k,j} = \boldsymbol{Y}^{brch}_{k,j} \cdot (\boldsymbol{V}_k - \boldsymbol{V}_j) \quad (6)$$

$$\Gamma_{k,j,\phi,n} = \frac{i^r_{k,j,\phi} S_n + i^i_{k,j,\phi}}{C_n} \quad (7)$$

$$\Gamma_{k,j,\phi,n} \le \overline{I_{k,J,\phi}} \quad (8)$$

$$\underline{V} \le \Psi_{k,\phi} \le \overline{V} \quad (9)$$

$$\Psi_{k,\phi} = \lambda Re\{v_{k,\phi}\} + \beta\left(Re\{v_{k,\phi}\} + |Im\{v_{k,\phi}\}|\right) \quad (10)$$

In the above the bold symbols refer to multi-phase complex components, while ϕ to one of the phases. Equation (4) describes the nodal current balance in complex form, where $\boldsymbol{Y}_{k,j}$ is the $N \times N$ admittance matrix of the branch connecting nodes k and j, being N the number of phases of the branch. Here, nodal complex currents injected by PODs, or individual distributed generating units (DG), or loads (D), if any, are defined as $\boldsymbol{I}^x_k$. Subset Ω_x is made of the elements x connected to bus k while subset Ω_B is made of the buses connected to bus k. The three-phase nodal voltage at the primary substation (PS) is the reference bus so it is fixed to the measured values. Equation (5) are linearized expressions for nodal injected power, where $\boldsymbol{V}^0_x$ terms are estimated values for the real and imaginary parts of the nodal voltages. They are first set by the initial, no flexibility activated, PF solution and then iteratively updated to the calculated value by optimization until they converge to a stable value. This usually occurs in 2-3 iterations and obtained results match an AC PF calculation. The left term of (5) is either fixed if the considered element does not have flexibility or imposed by linear equations (1)-(3). Branch currents are defined as $\boldsymbol{I}_{k,j}$ by (6), while (7) and (8) are the linearized maximum current branch constraints. Similarly, (9) and (10) give the linearized voltage limits constraints. The linearization is detailed in [17].

Optimization Model

If the market operates in **O1** logic, then the total cost of activated flexibility is minimized:

$$OF = \min\left\{\sum_{i_{POD}} \left[Y^z_{i_{POD}} \cdot \Delta^z_{0_{i_{POD}}} \cdot \pi^z_{0_{i_{POD}}}\right] + \sum_{i_{POD}} \sum_{i_{FX} \in\, i_{POD}} \left[P^z_{i_{FX}} \cdot \pi^z_{i_{FX}}\right]\right\} \quad (11)$$

In (11), parameters π_y^z, with $y = \{i_{POD}, 0_{i_{POD}}, i_{FX}\}$ and $z = \{UP, DW\}$, represent the prices in €/kWh associated to step of bided quantity. The first term of the objective function (OF) quantifies the total cost of discrete bid activation, while the second the total cost of continuous bid activation. If the market operates in **O2** logic and the total available flexibility from the LV network is required, then the total cost of activated flexibility needs to be maximized in one of the two directions, i.e. UP or DW:

$$OF = \max\left\{\sum_{i_{POD}}\left[Y_{i_{POD}}^z \cdot \Delta_{0_{i_{POD}}}^z \cdot \pi_{1_{i_{POD}}}^z\right] + \sum_{i_{POD}}\sum_{i_{FX}\in i_{POD}}\left[P_{i_{FX}}^z \cdot \pi_{i_{FX}}^z\right]\right\} \quad (12)$$

where z is either *UP* or *DW*.

Then, OF (11) or (12) is subjected to constraints (1)-(10) and a Mixed Integer Linear Problem (MILP) is obtained.

Finally, the MV DN needs to be symmetrical and balanced so the currents exchanged with the LV DN at PS need to be balanced. This is achieved by adding a penalty term quantifying the unbalance to the OF:

$$OF = \max\{OF + \pi^{unbal} \cdot (\overline{I_a^{PS}} + \overline{I_b^{PS}} + \overline{I_c^{PS}})\} \quad (13)$$

where π^{unbal} is the unbalance penalty cost equal to double the highest bided price and $\overline{I_{ph}^{PS}}$ are the phase currents produced by the slack generator (MV DN injection).

Constraints Filtering

Since POD flexibility is the only control variable and the LV DN topology is radial, constraints (7)-(10) are applied only to the network elements that can be influenced by flexibility variation to obtain model feasibility and size reduction:

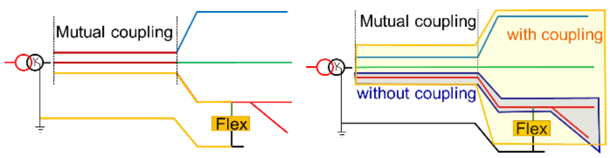

a. b.

Fig 3: Voltage and current bounds selection based on available flexibility: a. current bounds; b. voltage bounds.

- the flexibility can solve any current violation on the path between the PS and its location; as shown in Fig 3, *a*, flexibility can solve current violations only on its specific phases; if mutual couplings are present, violations in the coupled conductors can also be solved;
- the flexibility resource can solve any voltage violation in the nodes connected to the same MV/LV transformer through voltage drop control. With this assumption, concepts regarding mutual coupling introduced for current violations remain valid, as shown in Fig 3, *b*.

RESULTS

Input data

The proposed algorithm was applied on the IEEE 123 Nodes test feeder [18], represented in Fig 4. The demand was defined for one day with a resolution of 15 minutes using the demand shapes of [13] properly rescaled and distributed randomly and uniformly in the nodes. Each demand has been equipped with PV panels (with 14% assumed efficiency) dimensioned to cover 60% of the peak load and irradiation data from [20] related to Milan, Italy area for the day February 2nd, 2020. Simulations were carried out for the irradiation data of a summer day -July 22nd, 2020 [20]. Fig 5 shows the obtained aggregated power for the simulated day. Each load-PV panel pair was grouped under a POD that bids downward by decreasing continuously the PV production up to zero and upward by decreasing continuously the power absorbed up to 15% of the load. The flexibility activation cost was set at 0.2€/kWh, in line with the Italian Day-Ahead Market prices [20].

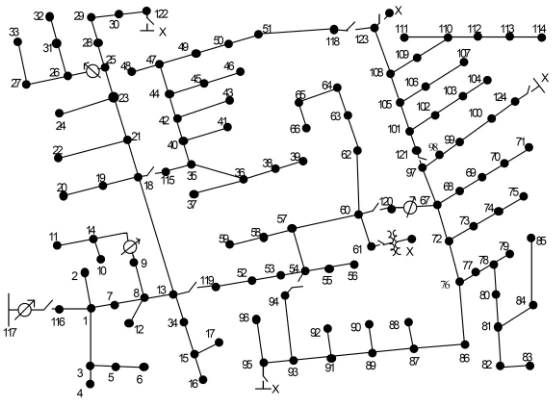

Fig 4: IEEE 123 Nodes test feeder [18].

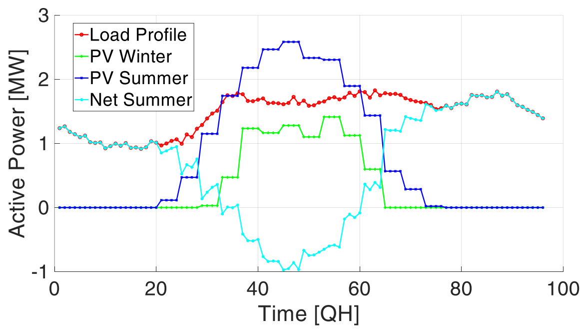

Fig 5: Aggregated load and PV power profiles.

The MILP optimization model was implemented in GAMS 38.3.0 and solved using CPLEX 12.6. Simulations were performed on a PC with Intel®Core™ i7-11390H CPU @ 3.40 GHz, RAM 16 GB.

Simulations

Four different studies were analyzed. First, option **O1** is considered and a current violation in phase *a* of line 76-86 is induced for the evening peak load period by considering the capacity rating of the conductor at 38A. Fig 6 shows the current profile in the congested line, while Fig 7 shows the activated flexibility in the congested quarters of hour. The violation is solved only by upward flexibility of PoDs below the congested conductor since this part of the feeder is made of uncoupled single-phase conductors, i.e. by

PODs in buses 86, 87, 88, 93, and 95 – see Fig 4. Moreover, since the bid price is equal for all PODs, the most technically efficient PODs are fully exploited, i.e. the ones closest to the congested conductor as they have the minimum effect on the real power losses between POD and congested conductor, hence the highest impact on the power transferred by congested conductor.

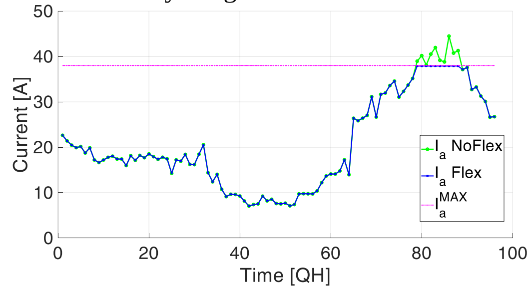

Fig 6: Current magnitude in phase a of line 76-86.

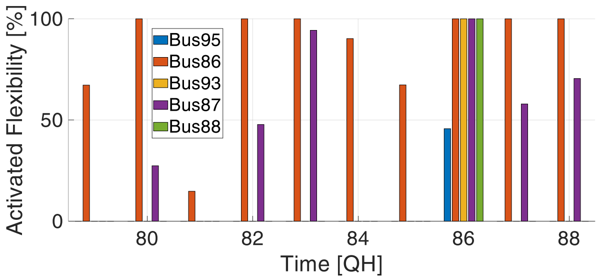

Fig 7: Line 76-86 congestion, activated flexibility per POD in %.

In the initial case, in the absence of voltage bounds the maximum voltage is in phase *a* of bus 119 and it reaches maximum values higher than 1.05 pu during the peak PV hours as the network operates in almost no-load conditions. Thus, in the second study option **O1** is considered, and the maximum voltage limit of this node is set at 1.05 p.u. Fig 8 shows that the violation is solved by activating flexibility. In details: (i) downward flexibility is activated only in phase *a* since flexibility in the mutually coupled phases is much less efficient in solving the violation and there is plenty available in phase *a*; (ii) flexibility is activated in the nodes most electrically distant from the violation (Fig.9) as they are the most efficient in solving the violation: activated downward flexibility increases the net demand hence it increases the currents in the largest portion of the network resulting in maximizing the voltage drop.

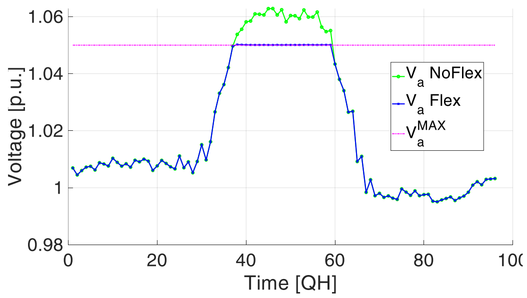

Fig 8: Bus 119 voltage before and after the flexibility activation.

In the third study, the balance constraint (12) in option **O1** is considered while current and voltage bounds are relaxed. Fig 10 shows the magnitude of the phase currents exchanged with the MV DN in the initial "Unbalanced" case and in the "Balanced" optimized case: the algorithm activates the flexibility required to balance the network.

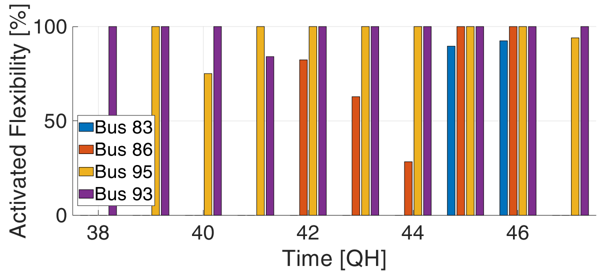

Fig 9: Bus 119 overvoltage, activated flexibility per POD in %

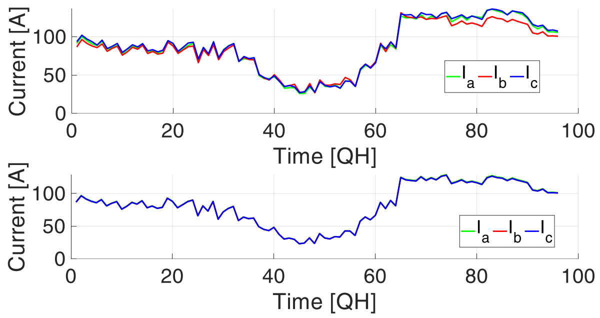

Fig 10: Primary Substation phase currents.

Fig 10 shows two different behaviors. Around the 55th quarter-of-hour, by minimizing the flexibility activation cost, flexibility is activated mainly on phase *b* by reducing PV output and bringing all three currents to the same value as those on phases *a* and *c*; this solution is certainly more economically advantageous than decreasing the load on phases *a* and *c*, since, in the latter case, the flexibility required would be about twice. Secondly, after the 75th quarter-of-hour (and, less obvious, in the morning periods) the behavior should be the same, but it can be seen that phase *b* does not change while the other two fall in line with it: during the night hours there is no PV production hence no downward bids to activate and increase the current in phase *b*; therefore the algorithm has to activate upward flexibility in phase *a* and *c* to balance the network.

Last, option **O2** is activated and the impact of the grid on the aggregated flexibility that can be provided to MV DN is evaluated. The aggregated flexibility is calculated at the level of PS by (12) and needs to be symmetrical: it is thus given by 3 times the minimum per-phase flexibility. To correctly obtain it, all previous constraints are activated, and the algorithm is first run in option **O1** to find a technically feasible operating point (FOP). Then, POD flexibility is recalculated quantitatively, and algorithm is run in option **O2** starting from the FOP: the technically feasible aggregated flexibility is thus evaluated with respect to the FOP. Fig 11 shows the results in terms of nominal quantities, which are the ones offered to the market, and the ones that are available due to the technical constraints of the grid, (i.e., by respecting all the voltage and currents constraints and by balancing the PS); the real quantities are lower than the nominal one, which means that not all the resources can be effectively used to solve congestions.

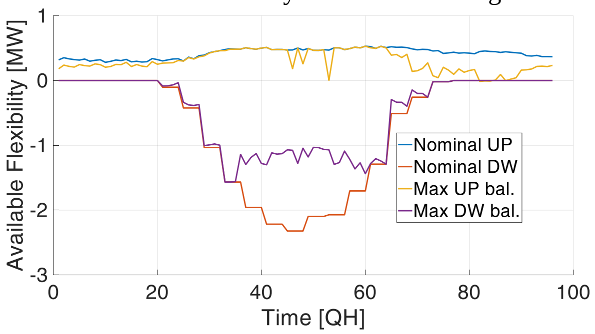

Fig 11: Comparison between nominal and actual flexibility.

CONCLUSIONS

In this paper a tool that optimally manages the flexibility in LV DN while guaranteeing grid security (balance network, voltage, and current bounds) is developed. As shown by simulations on a well-known test feeder, the tool can manage the flexibility locally to solve LV DN security problems or can also calculate the feasible aggregated flexibility to offer to a higher-level market. Future developments regard implementation of inter-temporal constraints to manage complex assets (like electrochemical storage) and advanced security constraints (like voltage ramps) and probabilistic aspects to better model RES uncertainty. At a practical level, the algorithm has been integrated within the DSO Technical Platform developed by Siemens Italy and successfully tested on the real network of Rome within the Italian Demo of the Platone European project [21].

REFERENCES

[1] M. Delfanti, A. Galliani, V. Olivieri, “The new role of DSOs: Ancillary services from RES towards a local dispatch”, *CIRED Workshop, Rome*, 11-12 June 2014.

[2] Italian Regulatory Authority for Electricity Gas and Water, Delibera 300/2017/R/eel, May 2017 (Italian only); Available online: Delibera300/2017.

[3] Z. Li, Q. Guo, H. Sun, J. Wang, "Coordinated transmission and distribution ac optimal power flow", *IEEE Trans. Smart Grid*, 2018, *9*, 1228–1240.

[4] C. Lin, W. Wu, M. Shahidehpour, 2019, "Decentralized ac optimal power flow for integrated transmission and distribution grids", *IEEE Trans. Smart Grid*, 11, 1–11.

[5] G. Migliavacca et al, 2017, "SmartNet: H2020 project analysing TSO- DSO interaction to enable ancillary services provision from distribution networks", *CIRED - Open Access Proceedings Journal*, (1), pp. 1998-2002.

[6] J.P. Chaves, M. Troncia, C.D. Silva, G. Willeghems, 2021, "Overview of market designs for the procurement of system services by DSOs and TSOs", *OneNet Deliverable 1.3*, Available online: OneNetD31.

[7] A. Delnooz, J. Vanschoenwinkel, E. Rivero, C. Madina, 2019, "Definition of scenarios and products for the demonstration Campaigns", *CoordiNet Deliverable 1.3*, Available online: CoordiNet.

[8] Falabretti D., Gulotta F., Siface D., 2023, “Scheduling and operation of RES-based virtual power plants with e-mobility: A novel integrated stochastic model”, *International Journal of Electrical Power and Energy Systems*, Vol. 144, January, 2023.

[9] R.Nebuloni. et al, 2023, “A hierarchical two-level MILP optimization model for the management of grid-connected BESS considering accurate physical model”, *Applied Energy*, Vol. 334, March 2023.

[10] Zhao, L., Zhang, W., Hao, H., Kalsi, K., 2017, “A geometric approach to aggregate flexibility modeling of thermostatically controlled loads”, *IEEE Trans. Power Syst.*, 2017, vol. 32, pp. 4721–4731.

[11] R. Singh, B. C. Pal, R. A. Jabr, R. B. Vinter, 2011, "Meter Placement for Distribution System State Estimation: An Ordinal Optimization Approach," *IEEE Trans. on Power Systems*, vol. 26, no. 4, pp. 2328-2335.

[12] Bovo C., Ilea V., Subasic M., Zanellini F., Arigoni C., Bonera R., 2014, “Improvement of observability in poorly measured distribution networks”, *Proceedings of 2014 Power Systems Computation Conference*, PSCC 2014, 18 – 22 August 2014, Wroclaw, Poland.

[13] Ilea V., et al, 2020, “Voltage control methodologies in active distribution networks”, *Energies*, Vol. 13, Issue 12, pp. 1-33.

[14] Arrigoni C. et al, “Smart distribution system the ingrid project and the evolution of supervision & control systems for smart distribution system management”, 2013, *AEIT Annual Conference 2013: Innovation and Scientific and Technical Culture for Development*, 3-5 October 2013, Milano, Italy.

[15] Arrigoni C. et al, 2016, “Smart Distribution Management System: Evolution of MV grids supervision & control systems”, *AEIT 2016 - International Annual Conference: Sustainable Development in the Mediterranean Area, Energy and ICT Networks of the Future*, 5-7 October 2016, Capri, Italy.

[16] G. Iannarelli, B. Greco, C. Moscatiello, A. Bosisio, C. Boccaletti, 2021, "The potential of urban PV generation in the Italian context of energy transition: a case study," *2021 AEIT International Annual Conference (AEIT)*, Milan, Italy, 2021, pp. 1-6

[17] J. S. Giraldo, P. P. Vergara, J. C. López, P. H. Nguyen, N. G. Paterakis, 2021, “A Linear AC-OPF Formulation for Unbalanced Distribution Networks”, *IEEE Trans. on Industry Applications*, vol. 57, 4462-4472.

[18] G. Dudgeon, 2023, “Distribution System Model in Simscape: 123 Node Test Feeder”, Available online: IEEE123.

[19] EU Science Lab, 2023, “PVGIS Online Tool”, available online: PVGIStool.

[20] Gestore Mercati Energetici, 2023, “Day-Ahead Market prices”, Available online: ItalyPX.

[21] PlatOne H2020 EU funded project (Grant No. 864300).